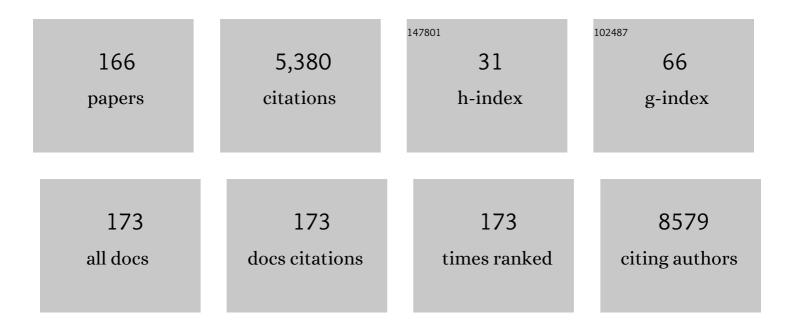
List of Publications by Year in descending order

Source: https://exaly.com/author-pdf/123274/publications.pdf Version: 2024-02-01



Υμε Ζηλο

#	Article	IF	CITATIONS
1	Development and validation of a parsimonious TB gene signature using the digital NanoString nCounter platform. Clinical Infectious Diseases, 2022, , .	5.8	2
2	Strongly Enhanced Growth of High-Temperature Superconducting Films on an Advanced Metallic Template. Crystal Growth and Design, 2022, 22, 2097-2104.	3.0	2
3	Study On Torsion Behavior of Superconducting Conductor On Round Core Cable. IEEE Transactions on Applied Superconductivity, 2022, 32, 1-5.	1.7	7
4	Quasi-Epitaxial Growth of β-Ga ₂ O ₃ -Coated Wide Band Gap Semiconductor Tape for Flexible UV Photodetectors. ACS Applied Materials & Interfaces, 2022, 14, 1304-1314.	8.0	29
5	Synergic realization of electrical insulation and mechanical strength in liquid nitrogen for high-temperature superconducting tapes with ultra-thin acrylic resin coating. Superconductor Science and Technology, 2022, 35, 075014.	3.5	26
6	Effect of Defects on the Quench Properties of Stacked REBCO Tapes. IEEE Transactions on Applied Superconductivity, 2021, 31, 1-5.	1.7	3
7	Analysis the water in aggregate glue droplets of spider orb web by TOFâ€&IMS. Surface and Interface Analysis, 2021, 53, 359-364.	1.8	1
8	<i>Ggps1</i> deficiency in the uterus results in dystocia by disrupting uterine contraction. Journal of Molecular Cell Biology, 2021, 13, 116-127.	3.3	6
9	Comparing tuberculosis gene signatures in malnourished individuals using the TBSignatureProfiler. BMC Infectious Diseases, 2021, 21, 106.	2.9	10
10	Highly Sensitive Low-Energy Laser Sensing Based on Sweep Pulse Excitation for Bolt Loosening Diagnosis. Journal of Nondestructive Evaluation, 2021, 40, 1.	2.4	4
11	animalcules: interactive microbiome analytics and visualization in R. Microbiome, 2021, 9, 76.	11.1	18
12	Ultra-fast growth (up to 100 nm s ^{â^'1}) of heavily doped EuBa ₂ Cu ₃ O ₇ film with highly aligned BaHfO ₃ nanocolumn structure. Superconductor Science and Technology, 2021, 34, 05LT01.	3.5	9
13	Geranylgeranyl pyrophosphate-mediated protein geranylgeranylation regulates endothelial cell proliferation and apoptosis during vasculogenesis in mouse embryo. Journal of Genetics and Genomics, 2021, 48, 300-311.	3.9	5
14	Ultra-fast growth of cuprate superconducting films: Dual-phase liquid assisted epitaxy and strong flux pinning. Materials Today Physics, 2021, 18, 100400.	6.0	56
15	Quantitative proteomics reveals arsenic attenuates stemâ€loop binding protein stability via a chaperone complex containing heat shock proteins and ERp44. Proteomics, 2021, 21, 2100035.	2.2	1
16	Genomic selection: A breakthrough technology in rice breeding. Crop Journal, 2021, 9, 669-677.	5.2	55
17	USP14 maintains HIF1-α stabilization via its deubiquitination activity in hepatocellular carcinoma. Cell Death and Disease, 2021, 12, 803.	6.3	24
18	Electromechanical Failure of NASICON-Type Solid-State Electrolyte-Based All-Solid-State Li-Ion Batteries. Chemistry of Materials, 2021, 33, 6841-6852.	6.7	14

#	Article	IF	CITATIONS
19	Numerical Study on Mechanical Properties of Conductors on Round Core Cables. IEEE Transactions on Applied Superconductivity, 2021, 31, 1-5.	1.7	20
20	Analysis and Validation of Human Targets and Treatments Using a Hepatocellular Carcinoma–Immune Humanized Mouse Model. Hepatology, 2021, 74, 1395-1410.	7.3	25
21	Type 2 diabetic mice enter a state of spontaneous hibernation-like suspended animation following accumulation of uric acid. Journal of Biological Chemistry, 2021, 297, 101166.	3.4	2
22	Sum frequency generation spectroscopy of the attachment disc of a spider. Spectrochimica Acta - Part A: Molecular and Biomolecular Spectroscopy, 2021, 263, 120161.	3.9	0
23	Building a sequence map of the pig pan-genome from multiple de novo assemblies and Hi-C data. Science China Life Sciences, 2020, 63, 750-763.	4.9	47
24	Cross-validation of existing signatures and derivation of a novel 29-gene transcriptomic signature predictive of progression to TB in a Brazilian cohort of household contacts of pulmonary TB. Tuberculosis, 2020, 120, 101898.	1.9	20
25	A Parsimonious Host Inflammatory Biomarker Signature Predicts Incident Tuberculosis and Mortality in Advanced Human Immunodeficiency Virus. Clinical Infectious Diseases, 2020, 71, 2645-2654.	5.8	11
26	Development of two-color resonant ionization sputtered neutral mass spectrometry and microarea imaging for Sr. Journal of Vacuum Science and Technology B:Nanotechnology and Microelectronics, 2020, 38, 044001.	1.2	3
27	Splicing factor PRPF6 upregulates oncogenic androgen receptor signaling pathway in hepatocellular carcinoma. Cancer Science, 2020, 111, 3665-3678.	3.9	10
28	Resonant sputtered neutral mass spectrometry using multiple reflections of laser to counterbalance Doppler broadening. Journal of Vacuum Science and Technology B:Nanotechnology and Microelectronics, 2020, 38, 034001.	1.2	0
29	Recent development and mass production of high <i>J</i> _e 2G-HTS tapes by using thin hastelloy substrate at Shanghai Superconductor Technology. Superconductor Science and Technology, 2020, 33, 074005.	3.5	17
30	USP22 positively modulates ERα action via its deubiquitinase activity in breast cancer. Cell Death and Differentiation, 2020, 27, 3131-3145.	11.2	26
31	Improvement of ionization yield in sputtered neutral mass spectrometry using pulsed infrared and ultraviolet lasers. Journal of Vacuum Science and Technology B:Nanotechnology and Microelectronics, 2020, 38, 034011.	1.2	3
32	The balance of protein farnesylation and geranylgeranylation during the progression of nonalcoholic fatty liver disease. Journal of Biological Chemistry, 2020, 295, 5152-5162.	3.4	19
33	Global Phosphoproteomic Analysis Reveals Significant Metabolic Reprogramming in the Termination of Liver Regeneration in Mice. Journal of Proteome Research, 2020, 19, 1788-1799.	3.7	6
34	Zoledronic acid inhibits TSC2-null cell tumor growth via RhoA/YAP signaling pathway in mouse models of lymphangioleiomyomatosis. Cancer Cell International, 2020, 20, 46.	4.1	7
35	BAP18 is involved in upregulation of CCND1/2 transcription to promote cell growth in oral squamous cell carcinoma. EBioMedicine, 2020, 53, 102685.	6.1	9
36	Liver governs adipose remodelling via extracellular vesicles in response to lipid overload. Nature Communications, 2020, 11, 719.	12.8	89

#	Article	IF	CITATIONS
37	Accumulation of cesium in glue balls of spiders' orb webs. Surface and Interface Analysis, 2020, 52, 569-572.	1.8	1
38	ASH2L is involved in promotion of endometrial cancer progression via upregulation of <i>PAX2</i> transcription. Cancer Science, 2020, 111, 2062-2077.	3.9	19
39	Generation of sub-half-cycle 10 µm pulses through filamentation at kilohertz repetition rates. Optics Express, 2020, 28, 36527.	3.4	8
40	G Protein–Coupled Receptor 30 Mediates the Anticancer Effects Induced by Eicosapentaenoic Acid in Ovarian Cancer Cells. Cancer Research and Treatment, 2020, 52, 815-829.	3.0	6
41	Differential effects of RASA3 mutations on hematopoiesis are profoundly influenced by genetic background and molecular variant. PLoS Genetics, 2020, 16, e1008857.	3.5	3
42	IKK-Mediated Regulation of the COP9 Signalosome via Phosphorylation of CSN5. Journal of Proteome Research, 2020, 19, 1119-1130.	3.7	9
43	Mass spectral database for TOF-SIMS of stable isotopes of Sr and Zr. Surface Science Spectra, 2020, 27, 025001.	1.3	0
44	Characterization of tantalum and tantalum nitride films on Ti6Al4V substrate prepared by filtered cathodic vacuum arc deposition for biomedical applications. Surface and Coatings Technology, 2019, 365, 24-32.	4.8	22
45	Egrâ€1 transcriptionally activates protein phosphatase PTP1B to facilitate hyperinsulinemiaâ€induced insulin resistance in the liver in type 2 diabetes. FEBS Letters, 2019, 593, 3054-3063.	2.8	10
46	Composite NASICON (Na ₃ Zr ₂ Si ₂ PO ₁₂) Solid-State Electrolyte with Enhanced Na ⁺ Ionic Conductivity: Effect of Liquid Phase Sintering. ACS Applied Materials & Interfaces, 2019, 11, 40125-40133.	8.0	115
47	Towards the Complete Goat Pan-Genome by Recovering Missing Genomic Segments From the Reference Genome. Frontiers in Genetics, 2019, 10, 1169.	2.3	29
48	Biodegradable Conducting Polymer Coating to Mitigate Early Stage Degradation of Magnesium in Simulated Biological Fluid: An Electrochemical Mechanistic Study. ChemElectroChem, 2019, 6, 4893-4901.	3.4	3
49	Large-scale ruminant genome sequencing provides insights into their evolution and distinct traits. Science, 2019, 364, .	12.6	266
50	Genetic basis of ruminant headgear and rapid antler regeneration. Science, 2019, 364, .	12.6	121
51	Loss of Phosphate Determines the Versatility of a Spider Orb-web Glue Ball. Analytical Sciences, 2019, 35, 645-649.	1.6	6
52	Improving the Flux Pinning With Artificial BCO Nanodots and Correlated Dislocations in YBCO Films Grown on IBAD-MgO Based Template. IEEE Transactions on Applied Superconductivity, 2019, 29, 1-5.	1.7	2
53	High-Speed Deposition of High-Performance REBCO Films by Using a Radiation Assisted Conductive Heating PLD System. IEEE Transactions on Applied Superconductivity, 2019, 29, 1-4.	1.7	5
54	Insight into the Interfacial Nucleation and Competitive Growth of YBa ₂ Cu ₃ O _{7â^Î} Films as High-Performance Coated Conductors by a Fluorine-Free Metal–Organic Decomposition Route. Crystal Growth and Design, 2019, 19, 6752-6762.	3.0	22

#	Article	IF	CITATIONS
55	Observation of spider silk by femtosecond pulse laser second harmonic generation microscopy. Surface and Interface Analysis, 2019, 51, 56-60.	1.8	5
56	Microstructure, mechanical and corrosion properties of electron-beam-melted and plasma-transferred arc-welded WCP/NiBSi metal matrix composites. Rare Metals, 2019, 38, 814-823.	7.1	12
57	Histone acetyltransferase MOF is involved in suppression of endometrial cancer and maintenance of ERα stability. Biochemical and Biophysical Research Communications, 2019, 509, 541-548.	2.1	8
58	Allele-specific expression and alternative splicing in horseè«onkey and cattleè® a k hybrids. Zoological Research, 2019, 40, 293-304.	2.1	18
59	Improvement of mapping quality by reflection of a laser beam in Resonance-SNMS. Journal of Surface Analysis (Online), 2019, 26, 204-205.	0.1	0
60	Changes of Calcium Distribution in Glue Ball of Spider's Orb-web under Low-temperature Stress. Journal of Surface Analysis (Online), 2019, 26, 220-221.	0.1	1
61	Influence of Seed Layer Materials on the Texture of IBAD-MgO Layer. IEEE Transactions on Applied Superconductivity, 2018, 28, 1-5.	1.7	2
62	Cytocompatible tantalum films on Ti6Al4V substrate by filtered cathodic vacuum arc deposition. Bioelectrochemistry, 2018, 122, 32-39.	4.6	16
63	Genomic variation in 3,010 diverse accessions of Asian cultivated rice. Nature, 2018, 557, 43-49.	27.8	1,091
64	Strategy of Diagnose the Issues Related to REBCO Films Deposited by a Reel-to-Reel PLD Process. IEEE Transactions on Applied Superconductivity, 2018, 28, 1-4.	1.7	4
65	Existing blood transcriptional classifiers accurately discriminate active tuberculosis from latent infection in individuals from south India. Tuberculosis, 2018, 109, 41-51.	1.9	51
66	Tribo-corrosion performance of filtered-arc-deposited tantalum coatings on Ti-13Nb-13Zr alloy for bio-implants applications. Wear, 2018, 400-401, 31-42.	3.1	27
67	Students' approaches to learning in a clinical practicum: A psychometric evaluation based on item response theory. Nurse Education Today, 2018, 66, 179-186.	3.3	5
68	Study on the Microstructure, Mechanical Properties and Corrosion Behavior of Mg-Zn-Ca Alloy Wire for Biomaterial Application. Journal of Materials Engineering and Performance, 2018, 27, 1837-1846.	2.5	29
69	Evidence for a role of geranylgeranylation in renal angiomyolipoma and renal epithelioid angiomyolipoma. Oncology Letters, 2018, 17, 1523-1530.	1.8	1
70	Geranylgeranyl diphosphate synthase (GGPPS) regulates nonâ€alcoholic fatty liver disease (NAFLD)–fibrosis progression by determining hepatic glucose/fatty acid preference under highâ€fat diet conditions. Journal of Pathology, 2018, 246, 277-288.	4.5	40
71	Exploring Host–Microbe Interactions in Lung Cancer. American Journal of Respiratory and Critical Care Medicine, 2018, 198, 1116-1118.	5.6	1
72	Ungerminated Rice Grains Observed by Femtosecond Pulse Laser Second-Harmonic Generation Microscopy. Journal of Physical Chemistry B, 2018, 122, 7855-7861.	2.6	2

#	Article	IF	CITATIONS
73	Novel Chromium-Free Technologies for the Prevention of Wet Stack Corrosion on Hot Dipped Metallic Coatings: A Review. Corrosion, 2018, 74, 918-935.	1.1	0
74	Evaluation of the Psychometric Properties of the Asian Adolescent Depression Scale and Construction of a Short Form: An Item Response Theory Analysis. Assessment, 2017, 24, 660-676.	3.1	9
75	Self-healing characteristic of praseodymium conversion coating on AZNd Mg alloy studied by scanning electrochemical microscopy. Electrochemistry Communications, 2017, 76, 6-9.	4.7	41
76	RPAN: rice pan-genome browser for â^1⁄43000 rice genomes. Nucleic Acids Research, 2017, 45, 597-605.	14.5	156
77	Influence of Substrate-Film Reactions on YBCO Grown by Fluorine-Free MOD Route. IEEE Transactions on Applied Superconductivity, 2017, 27, 1-4.	1.7	6
78	Impact of IRT item misfit on score estimates and severity classifications: an examination of PROMIS depression and pain interference item banks. Quality of Life Research, 2017, 26, 555-564.	3.1	10
79	Absorption, Distribution, Metabolism and Excretion of 3-MCPD 1-Monopalmitate after Oral Administration in Rats. Journal of Agricultural and Food Chemistry, 2017, 65, 2609-2614.	5.2	25
80	RNF8 identified as a co-activator of estrogen receptor α promotes cell growth in breast cancer. Biochimica Et Biophysica Acta - Molecular Basis of Disease, 2017, 1863, 1615-1628.	3.8	34
81	The hot deformation behavior and microstructure evolution of HA/Mg-3Zn-0.8Zr composites for biomedical application. Materials Science and Engineering C, 2017, 77, 690-697.	7.3	23
82	EUPAN enables pan-genome studies of a large number of eukaryotic genomes. Bioinformatics, 2017, 33, 2408-2409.	4.1	47
83	A Validated and Reliable Instrument Investigating Engineering Students' Perceptions of Competency in Generic Skills. Journal of Engineering Education, 2017, 106, 299-325.	3.0	59
84	Mechanism of ionic conduction in multi-layer polymeric films studied via electrochemical measurement and theoretical modelling. Progress in Organic Coatings, 2017, 108, 68-74.	3.9	1
85	Corrosion behaviour and microstructure of tantalum film on Ti6Al4V substrate by filtered cathodic vacuum arc deposition. Thin Solid Films, 2017, 636, 54-62.	1.8	22
86	Measuring Longitudinal Gains in Student Learning: A Comparison of Rasch Scoring and Summative Scoring Approaches. Research in Higher Education, 2017, 58, 605-616.	1.7	6
87	Zoledronic acid, an FPPS inhibitor, ameliorates liver steatosis through inhibiting hepatic de novo lipogenesis. European Journal of Pharmacology, 2017, 814, 169-177.	3.5	17
88	Comparing perceived learning experiences of two concurrent cohorts under curriculum reform in Hong Kong. Quality Assurance in Education, 2017, 25, 270-286.	1.5	1
89	Preparation and characterization of polypropylene/noble metal nanocomposites based on reactor granule technology. Polymer, 2017, 127, 251-258.	3.8	7
90	Mechanical properties of TiN ceramic coating on a heat treated Ti-13Zr-13Nb alloy. Journal of Alloys and Compounds, 2017, 724, 34-44.	5.5	6

#	Article	IF	CITATIONS
91	Second-order nonlinear optical microscopy of spider silk. Applied Physics B: Lasers and Optics, 2017, 123, 1.	2.2	15
92	Comparing five depression measures in depressed Chinese patients using item response theory: an examination of item properties, measurement precision and score comparability. Health and Quality of Life Outcomes, 2017, 15, 60.	2.4	17
93	Electric Field Effect on Optical Second-harmonic Generation of Amphoteric Megamolecule Aggregates. Journal of the Physical Society of Japan, 2017, 86, 124401.	1.6	3
94	Practical Consequences of Item Response Theory Model Misfit in the Context of Test Equating with Mixed-Format Test Data. Frontiers in Psychology, 2017, 8, 484.	2.1	15
95	Optical second-harmonic images of sacran megamolecule aggregates. Journal of the Optical Society of America A: Optics and Image Science, and Vision, 2017, 34, 146.	1.5	8
96	Psychometric properties of the Children's Response Styles Questionnaire in a Hong Kong Chinese community sample. Health and Quality of Life Outcomes, 2017, 15, 198.	2.4	8
97	The Influence of Zn Content on the Corrosion and Wear Performance of Mg-Zn-Ca Alloy in Simulated Body Fluid. Journal of Materials Engineering and Performance, 2016, 25, 3890-3895.	2.5	44
98	BAP18 coactivates androgen receptor action and promotes prostate cancer progression. Nucleic Acids Research, 2016, 44, 8112-8128.	14.5	28
99	In situ evaluation of corrosion damage using non-destructive electrochemical measurements—A case study. Journal of Industrial and Engineering Chemistry, 2016, 43, 36-43.	5.8	19
100	Mitigation of 3-Monochloro-1,2-propanediol Ester Formation by Radical Scavengers. Journal of Agricultural and Food Chemistry, 2016, 64, 5887-5892.	5.2	44
101	Formation of 3-MCPD Fatty Acid Esters from Monostearoyl Glycerol and the Thermal Stability of 3-MCPD Monoesters. Journal of Agricultural and Food Chemistry, 2016, 64, 8918-8926.	5.2	32
102	Tribological behavior of hydrogenated diamond-like carbon on polished alumina substrate with chromium interlayer for biomedical application. Biotribology, 2016, 7, 1-10.	1.9	12
103	Corrosion behaviour and adhesion properties of sputtered tantalum coating on Ti6Al4V substrate. Surface and Coatings Technology, 2016, 307, 666-675.	4.8	48
104	SNF5 is Involved in Suppression of Hepatocellular Carcinoma Progression via TGFâ€Beta 1 Signaling. Anatomical Record, 2016, 299, 869-877.	1.4	7
105	Surface modification of a Ti2AlC soft ceramic by plasma nitriding treatment. Surface and Coatings Technology, 2015, 281, 164-168.	4.8	6
106	MDC1 Enhances Estrogen Receptor-mediated Transactivation and Contributes to Breast Cancer Suppression. International Journal of Biological Sciences, 2015, 11, 992-1005.	6.4	32
107	Corrosion degradation behavior of Mg–Ca alloy with high Ca content in SBF. Transactions of Nonferrous Metals Society of China, 2015, 25, 3339-3347.	4.2	27
108	Mono- and multiple TiN(/Ti) coating adhesion mechanism on a Ti–13Nb–13Zr alloy. Applied Surface Science, 2015, 355, 502-508.	6.1	34

#	Article	IF	CITATIONS
109	Upregulation of miR-125b by estrogen protects against non-alcoholic fatty liver in female mice. Journal of Hepatology, 2015, 63, 1466-1475.	3.7	79
110	Preparation of monodispersed CuS nanocrystals in an oleic acid/paraffin system. RSC Advances, 2015, 5, 84465-84470.	3.6	15
111	MDC1 functionally identified as an androgen receptor co-activator participates in suppression of prostate cancer. Nucleic Acids Research, 2015, 43, 4893-4908.	14.5	47
112	The effect of anodized Ti on output performance of biomedical compatible triboelectric nanogenerators used for controlling the degradation of Mg-3wt%Zn-0.8wt%Zr. Nanotechnology, 2015, 26, 495401.	2.6	4
113	Nanomechanical properties of TiCN and TiCN/Ti coatings on Ti prepared by Filtered Arc Deposition. Materials Science & Engineering A: Structural Materials: Properties, Microstructure and Processing, 2015, 625, 56-64.	5.6	32
114	Effects of heat–moisture treatment reaction conditions on the physicochemical and structural properties of maize starch: Moisture and length of heating. Food Chemistry, 2015, 173, 1125-1132.	8.2	96
115	Effect of extreme pressure agents on the anti-scratch behaviour of high-speed steel material. Tribology International, 2015, 81, 19-28.	5.9	15
116	p300-Dependent Acetylation of Activating Transcription Factor 5 Enhances C/EBPβ Transactivation of C/EBPα during 3T3-L1 Differentiation. Molecular and Cellular Biology, 2014, 34, 315-324.	2.3	28
117	Suv39h1 Mediates AP-2α-Dependent Inhibition of C/EBPα Expression during Adipogenesis. Molecular and Cellular Biology, 2014, 34, 2330-2338.	2.3	35
118	Effect of corrosion on mechanical behaviors of Mg-Zn-Zr alloy in simulated body fluid. Frontiers of Materials Science, 2014, 8, 264-270.	2.2	26
119	Synthesis of tunable ZnS–CuS microspheres and visible-light photoactivity for rhodamine B. New Journal of Chemistry, 2014, 38, 4182-4189.	2.8	49
120	X-ray diffraction stress analysis of interrupted titanium nitride films: Combining the sin2Ï^ and crystallite group methods. Thin Solid Films, 2014, 562, 206-210.	1.8	8
121	The mechanical behaviour of TiN and multi-layered coating of TiN/Ti on Ti6Al4V substrate during nano-indentation. International Journal of Surface Science and Engineering, 2014, 8, 95.	0.4	4
122	Preparation of various kinds of copper sulfides in a facile way and the enhanced catalytic activity by visible light. Journal of Materials Chemistry A, 2013, 1, 8616.	10.3	61
123	Preparation of spherical ZnO/ZnS core/shell particles and the photocatalytic activity for methyl orange. Materials Letters, 2013, 96, 221-223.	2.6	26
124	Aqueous Colloidal Stability Evaluated by Zeta Potential Measurement and Resultant <scp><scp>TiO</scp></scp> 2 for Superior Photovoltaic Performance. Journal of the American Ceramic Society, 2013, 96, 2636-2643.	3.8	26
125	Morphology-controllable 1D–3D nanostructured TiO2bilayer photoanodes for dye-sensitized solar cells. Chemical Communications, 2013, 49, 966-968.	4.1	94
126	Identification of endocrine disrupting chemicals activating SXR-mediated transactivation of CYP3A and CYP7A1. Molecular and Cellular Endocrinology, 2013, 365, 36-43.	3.2	6

#	Article	IF	CITATIONS
127	Studies of the Surface Reaction Mechanisms of Pb-3 wt%Sn-0.5 wt%Ag Anode in CrO ₃ Solutions. Journal of the Electrochemical Society, 2013, 160, E60-E66.	2.9	6
128	Structurally stabilized mesoporous TiO2 nanofibres for efficient dye-sensitized solar cells. APL Materials, 2013, 1, .	5.1	22
129	G9a is transactivated by C/EBPβ to facilitate mitotic clonal expansion during 3T3-L1 preadipocyte differentiation. American Journal of Physiology - Endocrinology and Metabolism, 2013, 304, E990-E998.	3.5	25
130	SYNTHESIS OF NANOCRYSTALLINE CdS QUANTUM DOTS VIA PARAFFIN LIQUID AS SOLVENT AND OLEIC ACID AS THE REACTING MEDIA. International Journal of Nanoscience, 2012, 11, 1240038.	0.7	2
131	Surface engineering of biaxial Gd2Zr2O7 thin films deposited on Ni–5at%W substrates by a chemical solution method. CrystEngComm, 2012, 14, 3089.	2.6	9
132	Pinning Properties of PLD (NdxSmxGd1â^'2x)Ba2Cu3O7â^'δ Thin films. Physics Procedia, 2012, 36, 463-467.	1.2	0
133	Continually adjustable oriented 1D TiO2 nanostructure arrays with controlled growth of morphology and their application in dye-sensitized solar cells. CrystEngComm, 2012, 14, 5472.	2.6	32
134	Improved photovoltaic performance of dye-sensitized solar cells with modified self-assembling highly ordered mesoporous TiO2 photoanodes. Journal of Materials Chemistry, 2012, 22, 11711.	6.7	37
135	Rational Design of 3D Dendritic TiO ₂ Nanostructures with Favorable Architectures. Journal of the American Chemical Society, 2011, 133, 19314-19317.	13.7	387
136	Characterization and properties of an advanced composite substrate for YBCO-coated conductors. Acta Materialia, 2010, 58, 1299-1308.	7.9	19
137	Silicon/Single-Walled Carbon Nanotube Composite Paper as a Flexible Anode Material for Lithium Ion Batteries. Journal of Physical Chemistry C, 2010, 114, 15862-15867.	3.1	128
138	Development of Advanced Substrates for HTS Coated Conductors. IEEE Transactions on Applied Superconductivity, 2010, 20, 1569-1572.	1.7	7
139	Fabrication and Superconducting Properties of Highly Dense \${m MgB}_{2}\$ Bulk Using a Two-Step Sintering Method. IEEE Transactions on Applied Superconductivity, 2009, 19, 2763-2766.	1.7	7
140	Superconducting Properties of \${m MgB}_{2}\$ Wire Using Ball-Milled Low Purity Boron. IEEE Transactions on Applied Superconductivity, 2009, 19, 2714-2717.	1.7	0
141	Investigation of Texture Formation in Ni-7at.%W Alloy Substrates by Spark Plasma Sintering Technique. IEEE Transactions on Applied Superconductivity, 2009, 19, 3279-3282.	1.7	4
142	YBCO Films With \${m Zr}^{4+}\$ Doping Grown by MOD Method. IEEE Transactions on Applied Superconductivity, 2009, 19, 3403-3406.	1.7	2
143	Preparation of \${m CeO}_{2}/{m La}_{2}{m Zr}_{2}{m O}_{7}\$ Buffer Layers on Textured Ni5W Substrates by Chemical Solution Deposition Method. IEEE Transactions on Applied Superconductivity, 2009, 19, 3423-3426.	1.7	7
144	A simple MOD method to grow a single buffer layer of Ce0.8Gd0.2O1.9 (CGO) for coated conductors. Physica C: Superconductivity and Its Applications, 2009, 469, 230-233.	1.2	7

#	Article	IF	CITATIONS
145	Study on Ce _x La _{1-x} O ₂ Buffer Layer used in Coated Conductors by Chemical Solution Method. Wuji Cailiao Xuebao/Journal of Inorganic Materials, 2009, 24, 1201-1204.	1.3	13
146	Technique for developing highly strengthened and biaxially textured composite substrates for coated superconductor tapes. Acta Materialia, 2008, 56, 23-30.	7.9	17
147	A TFTC/STAGA Module Mediates Histone H2A and H2B Deubiquitination, Coactivates Nuclear Receptors, and Counteracts Heterochromatin Silencing. Molecular Cell, 2008, 29, 92-101.	9.7	331
148	Effect of addition of TiO <inf>2</inf> /SiO <inf>2</inf> nanoparticles on H <inf>c2</inf> and H <inf>irr</inf> in MgB <inf>2</inf> bulks. , 2008, , .		0
149	Preparation and properties of YSZ-doped YBCO films grown by the TFA-MOD method. Superconductor Science and Technology, 2008, 21, 115012.	3.5	9
150	Fabrication of Reinforced and Biaxially Textured NiW Alloy Substrates by Spark Plasma Sintering Technique. IEEE Transactions on Applied Superconductivity, 2007, 17, 3424-3427.	1.7	2
151	High Critical Current Densities in SiC Doped In-Situ\${hbox{MgB}}_{2}\$ Wires Prepared by Continuous Tube Forming and Filling Technique. IEEE Transactions on Applied Superconductivity, 2007, 17, 2822-2825.	1.7	14
152	Kinetic roughening of magnetic flux penetration in MgB2 thin films. Applied Physics Letters, 2007, 91, 222505.	3.3	2
153	Deposition of Biaxially Textured \${m CeO}_{2}\$ Thin Films on Single Crystal and Textured Ni5W Substrates Using Solution Derived Method. IEEE Transactions on Applied Superconductivity, 2007, 17, 3440-3442.	1.7	8
154	Preparation of Cube Textured Ni5W/Ni9W Composite Substrate for YBCO Coated Conductors. IEEE Transactions on Applied Superconductivity, 2007, 17, 3420-3423.	1.7	10
155	\${hbox{MgB}}_{2}\$ for Application to RF Cavities for Accelerators. IEEE Transactions on Applied Superconductivity, 2007, 17, 1330-1333.	1.7	22
156	Study of Oxygen Incorporation in PLD \${m MgB}_{2}\$ Films by Rutherford Backscattering Spectroscopy. IEEE Transactions on Applied Superconductivity, 2007, 17, 2875-2878.	1.7	3
157	Highly reinforced and cube textured Ni alloy composite substrates by a hybrid route. Acta Materialia, 2007, 55, 2609-2614.	7.9	33
158	A novel technique for developing composite substrates used in YBCO coated conductors. Scripta Materialia, 2007, 56, 129-131.	5.2	12
159	Off-axis MgB2films using anin situannealing pulsed laser deposition method. Superconductor Science and Technology, 2005, 18, 395-399.	3.5	15
160	Superconducting and Microstructural Properties of Two Types of <tex>\$rm MgB_2\$</tex> Films Prepared by Pulsed Laser Deposition. IEEE Transactions on Applied Superconductivity, 2005, 15, 3261-3264.	1.7	10
161	Comparative study ofin situandex situMgB2films prepared by pulsed laser deposition. Superconductor Science and Technology, 2004, 17, S482-S485.	3.5	21
162	In situannealing of superconducting MgB2films prepared by pulsed laser deposition. Superconductor Science and Technology, 2003, 16, 1487-1492.	3.5	19

#	Article	IF	CITATIONS
163	Activation Function-1 Domain of Androgen Receptor Contributes to the Interaction between Subnuclear Splicing Factor Compartment and Nuclear Receptor Compartment. Journal of Biological Chemistry, 2002, 277, 30031-30039.	3.4	46
164	Study on Functions of Chrome and Fluoride lons in Plating Process of Tin Free Steel by Means of Cyclic Voltammetry. Materials Science Forum, 0, 773-774, 557-562.	0.3	0
165	Deformation Behavior and Wear Resistance of Hard TiCN and TiCN/Ti Coatings on Ti6Al4V Alloy. Advanced Materials Research, 0, 939, 451-458.	0.3	1
166	Study on Simulation and Experiment of Micro Sheet Metal Forming. Advanced Materials Research, 0, 941-944, 1876-1881.	0.3	2